

## Global search in photoelectron diffraction structure determination using genetic algorithms

This article has been downloaded from IOPscience. Please scroll down to see the full text article.

2007 J. Phys.: Condens. Matter 19 446002

(<http://iopscience.iop.org/0953-8984/19/44/446002>)

View [the table of contents for this issue](#), or go to the [journal homepage](#) for more

Download details:

IP Address: 129.252.86.83

The article was downloaded on 29/05/2010 at 06:29

Please note that [terms and conditions apply](#).

## Global search in photoelectron diffraction structure determination using genetic algorithms

M L Viana<sup>1,2</sup>, R Díez Muiño<sup>2,3</sup>, E A Soares<sup>1</sup>, M A Van Hove<sup>4</sup> and V E de Carvalho<sup>1</sup>

<sup>1</sup> Departamento de Física, Icx, UFMG, Belo Horizonte, Minas Gerais, Brazil

<sup>2</sup> Donostia International Physics Center DIPC, Paseo Manuel de Lardizabal 4, 20018 San Sebastián, Spain

<sup>3</sup> Centro de Física de Materiales, Centro Mixto CSIC-UPV/EHU, Paseo Manuel de Lardizabal 3, 20018 San Sebastián, Spain

<sup>4</sup> Department of Physics and Materials Science, City University of Hong Kong, Hong Kong

Received 22 June 2007, in final form 27 July 2007

Published 24 September 2007

Online at [stacks.iop.org/JPhysCM/19/446002](http://stacks.iop.org/JPhysCM/19/446002)

### Abstract

Photoelectron diffraction (PED) is an experimental technique widely used to perform structural determinations of solid surfaces. Similarly to low-energy electron diffraction (LEED), structural determination by PED requires a fitting procedure between the experimental intensities and theoretical results obtained through simulations. Multiple scattering has been shown to be an effective approach for making such simulations. The quality of the fit can be quantified through the so-called R-factor. Therefore, the fitting procedure is, indeed, an R-factor minimization problem. However, the topography of the R-factor as a function of the structural and non-structural surface parameters to be determined is complex, and the task of finding the global minimum becomes tough, particularly for complex structures in which many parameters have to be adjusted. In this work we investigate the applicability of the genetic algorithm (GA) global optimization method to this problem. The GA is based on the evolution of species, and makes use of concepts such as crossover, elitism and mutation to perform the search. We show results of its application in the structural determination of three different systems: the Cu(111) surface through the use of energy-scanned experimental curves; the Ag(110)-c(2 × 2)-Sb system, in which a theory-theory fit was performed; and the Ag(111) surface for which angle-scanned experimental curves were used. We conclude that the GA is a highly efficient method to search for global minima in the optimization of the parameters that best fit the experimental photoelectron diffraction intensities to the theoretical ones.

(Some figures in this article are in colour only in the electronic version)

## 1. Introduction

Photoelectron diffraction [1, 2] (PED) is one of the most widely used experimental techniques in surface atomic structural determination. Core-level electrons of the surface atoms are excited by photons typically in the x-ray range and are scattered by the nearby surface atoms before reaching the detector [1]. The diffracted intensities, usually measured as a function of the photoelectron momentum (kinetic energy) and/or the angles between the analyzer and the sample, contain rich information about the structural and non-structural surface parameters. Theoretical simulations are required to extract those parameter values, because no direct method is available to reliably and accurately determine those parameters. (More or less direct holographic methods can produce less accurate results, but not reliably and not for all surfaces [3].)

Multiple scattering (MS) theory is a computationally effective method to simulate photoelectron diffraction patterns [4]. The MS method calculates the photoelectron diffraction pattern as the coherent sum of the direct unscattered photoemission wave and the interference contributions resulting from the MS of the direct wave with bulk and surface atoms. In most cases, the solid is represented by a cluster of non-overlapping spherical muffin-tin potentials. The diffraction pattern thus calculated obviously depends on the particular structural parameters used to represent the system.

Several codes based on this method have been developed to make such simulations, such as MSPHD [5], PAD [6], EDAC [7, 8], and MSCD [9]. Among them, let us briefly describe the code we have used for the present calculations, namely the MSCD package. MSCD stands for multiple scattering calculation of diffraction. It is a versatile and efficient code designed to simulate photoelectron diffraction patterns in core-level photoemission from surfaces. The code is based on MS calculations of the photoelectron patterns [10]. The Rehr–Albers separable representation of spherical-wave propagators is used [11], and several fitting procedures are available to obtain structural information on the system under study. Inelastic scattering of electrons in their path inside the solid is taken into account in a phenomenological way. Thermal vibrational effects are included using a Debye–Waller-type attenuation factor. The crossing of the surface is modeled by a square-step potential barrier. Energy scans as well as angular scans are easily calculated with this program.

In general, the agreement between calculated and experimental curves in the fitting process is quantified through the so-called R-factor [10]. Hence, the structural determination becomes an R-factor minimization problem. However, the R-factor topography presents, in general, many local minima, so it is necessary to address the difficult problem of identifying the global minimum. This is particularly true for complex systems, such as compound, reconstructed and adsorbate-covered surfaces.

In the context of low-energy electron diffraction (LEED), which is similar to photoelectron diffraction in its purpose and approach to solving surface structure, several schemes have been explored for finding the global minimum: pattern search methods [12], simulated annealing [13], fast simulated annealing [14–16], a modified random sampling algorithm [17] and genetic algorithms [18].

In this paper, we present an implementation of the genetic algorithm (GA) procedure [18, 19] to numerically solve the problem of finding the global minimum in the multidimensional R-factor surface. The GA is a global optimization method based on the evolution of species. The MSCD package is used to calculate the photoelectron diffraction curves required in the optimization process. We have tested our procedure with three different systems: (i) a clean Cu(111) surface, in which experimental energy scans are available, and five fitting parameters were optimized; (ii) Ag(110)–c(2 × 2)–Sb, for which ‘pseudo-experimental’

angular scans were generated by simulations using the MSCD code for the correct surface structure found by Nascimento *et al* [20], with six structural parameters being fitted; and (iii) Ag(111), for which experimental angle scans are available, and five parameters were optimized. We have focused on the methodological aspects of the implementation, although brief discussions of the resulting structural parameters of the surfaces mentioned are included as well. Our conclusion is that the GA is a highly efficient method to search global minima in the R-factor hypersurface, and thus to optimize the parameters that best fit experimental photoelectron diffraction curves.

The paper is organized as follows. In section 2, the implementation is described. In section 3, we show methodological results of several performance tests. In section 4, we discuss the physical results obtained for the three tested systems, and include the fitted values obtained for parameters such as interlayer spacing, variations of length of the surface unit cell vectors, Debye temperature and inner potential. Section 5 includes a summary and the conclusions of our work.

## 2. Implementation of the genetic algorithm method

### 2.1. General description of genetic algorithms

Genetic algorithms (GAs) form a class of a global search methods based on the evolution of species. In the same way that living creatures change their fitness over time so as to better adapt to the environment, the set of parameters in an optimization problem can evolve to become a more adequate solution.

Many optimization methods are based on some form of ‘steepest descent’ [19]: they typically start from a unique trial solution, and use function derivatives to decide on the search direction. Numerical algorithms of this type usually converge to the nearest local minimum, and there is no guarantee that the reached minimum is the global minimum of the function. By contrast, a GA works with populations of solutions, starting the search from many different trial solutions, comparing their function values and then generating new trial solutions that may exist in very different parts of parameter space. Thus, it is able to roam throughout parameter space and look for the global minimum.

A given surface structure is defined by a set of particular parameters and is treated as an individual that is coded into a string of binary or real numbers, like chromosomes in living organisms [18, 19]: the string completely defines the structure in question. A GA population contains a pre-determined number of individuals, each characterized by its own binary or real string. The initial population is often chosen randomly, although the actual values of the parameters should be within a reasonable range. Search operators, or evolutionary devices, act on the population: they choose some individuals to participate in crossover, elitism and mutation processes.

The main GA search device is the crossover. In this process, pairs of individuals are chosen to act as parents that will produce two children each for the next generation. Within each pair, the two strings are typically cut in two pieces at a randomly chosen point and the pieces from each parent exchanged to form two new mixed strings, the children. Thus a string AB and a string YZ can become a string AZ and a string YB.

The hope is that at least one of the two new crossed-over strings will combine the ‘good’ features of the two parents and thus will be ‘better’ than either parent. To bias the search in this direction, one adds evolutionary pressure toward improved children. This is achieved mainly by selecting parents that have a relatively high level of fitness (i.e. a relatively good R-factor in our case).

Individuals generated by crossover present, in general, a better fitness than their ‘parents’, but not always. The use of elitism or ‘cloning’ secures the survival of the best individual (or individuals) from one generation to the next, by simply copying them into the next generation: this avoids the risk of losing a good solution.

Mutation is commonly added to prevent the situation where all individuals of the population are trapped in local minima: by randomly choosing some individuals from every generation and changing, randomly again, some of the bits in their strings, these individuals are modified and thus sent into random parts of parameter space. A ‘mutation rate’ is initially chosen to determine how often the mutation device will act.

It should be noted that many variations of these processes have been proposed, hence the plural designation ‘genetic algorithms’.

## 2.2. Codification

In the present implementation, our goal is to find a surface structural parameter set that minimizes the R-factor. In other words, we look for the calculated intensity curves that offer the best fit to the experimental curves. The agreement between the curves is measured through an R-factor which is defined as [10]

$$R = \frac{\sum_{i=1}^N (\chi_{ci} - \chi_{ei})^2}{\sum_{i=1}^N (\chi_{ci}^2 + \chi_{ei}^2)}, \quad (1)$$

where  $\chi_{ci}$  and  $\chi_{ei}$  are calculated and experimental  $\chi$  curves (i.e. normalized intensities), respectively. The  $\chi$  function is defined [10] as  $\chi(\theta, \phi, K) = \frac{I(\theta, \phi, K) - I_0(\theta, \phi, K)}{I_0(\theta, \phi, K)}$ , where  $I(\theta, \phi, K)$  is the photoelectron intensity as a function of the polar ( $\theta$ ) and azimuthal ( $\phi$ ) angles and the kinetic energy  $K$ , and  $I_0(\theta, \phi, K)$  is the background intensity equal to the free atomic photoemission cross-section. The index  $i$  refers to the set of parameters,  $\theta$ ,  $\phi$ , and  $K$ , corresponding to the intensity point. In this way, the value  $N$  corresponds to the total number of points, which is equal to the number of  $\theta$  times the number of  $\phi$  times the number of  $K$ . We refer each trial structure to the ideally terminated bulk structure. In the case of adsorbate layers the adsorbate atoms are placed according to the unit cell shown by the LEED pattern, and their interlayer distances are usually taken to be the same as those of the substrate spacings (for atoms with very different radii, one would make other choices). Then we search for the set of displacements which minimize the R-factor. Thus, each individual of the population represents a set of displacements that must be added to the respective bulk atomic coordinate. The codification, required in the GA, was made through binary and real strings. For the simple systems Cu(111) and Ag(111) we used the binary or classical codification. In this kind of codification a given individual coordinate displacement (corresponding to one parameter to be optimized) is coded in one *segment* of the full binary string that represents an individual. The first bit of this segment represents the arithmetic sign of this displacement, while the remaining bits of this segment represent its magnitude, as follows. Those remaining bits represent an integer number. When all those bits are equal to 1 (one), the displacement is maximal: this maximum value represents the largest physical displacement that we allow for this coordinate. The ratio of the current value of this binary string segment to its maximum possible value is the current displacement. Table 1 shows a typical binary string for an individual in a situation where three parameters are optimized using eight bits for each of them. The first bit in each segment, written in bold face, gives the sign of the displacement. The last seven bits represent integer numbers in the range of 0–127, shown in the second row. Equation (2) shows how the physical displacement is calculated, if the value  $\Delta X_{i_{\max}}$  is the maximum displacement allowed for the coordinate  $i$ . The number of bits in the representation can be increased if a higher accuracy is required.

**Table 1.** Typical binary string, ‘chromosome’, for an individual in a problem where three parameters are optimized.

10 001 100	00 110 011	11 001 110
+12	−51	+78

**Table 2.** Typical real string representation or ‘chromosome’, for an individual in a problem where three parameters are optimized.

Real string	Physical displacement
−0.237	$\Delta X_1 = -0.237 \times \Delta X_{1_{\max}}$
+0.866	$\Delta X_2 = +0.866 \times \Delta X_{2_{\max}}$
+0.148	$\Delta X_3 = +0.148 \times \Delta X_{3_{\max}}$

For the Ag(110)–c(2 × 2)–Sb system we used a codification with real numbers. Here the string is formed by real numbers with values lying in the range from −1 to 1. The physical displacement is equal to its corresponding real value in the string times a maximum allowed displacement. Table 2 shows how the real representation works.

$$\begin{aligned}
 \Delta X_1 &= +\frac{12}{127} \times \Delta X_{1_{\max}} \\
 \Delta X_2 &= -\frac{51}{127} \times \Delta X_{2_{\max}} \\
 \Delta X_3 &= +\frac{78}{127} \times \Delta X_{3_{\max}}.
 \end{aligned} \tag{2}$$

Both codifications are suitable for the PED structural determination problem. However, the real codification does not require binary–decimal and decimal–binary encoding steps in the algorithm and thus can speed up the calculation.

### 2.3. Step-by-step application of the GA to MSCD

Our implementation of the GA method for the photoelectron diffraction problem in the MSCD code follows the general steps described below to determine the structural and non-structural surface parameters, and is schematically illustrated in figure 1.

- (i) An initial population of  $N$  individuals is chosen ( $N$  is an even number). Each individual is a vector containing the  $P$  parameters to be optimized in the surface analysis of the system. The value of each parameter is randomly chosen within a physically acceptable range for that system. Each individual is coded as described in section 2.2 and its binary or real string contains the displacements to be added to the parameters of a reference initial surface structure.
- (ii) The MSCD code calculates the theoretical photoelectron intensity curves for one individual, which we call individual I. It starts from general information available about the system, such as atomic phase shifts, radial matrices for the emitter atoms, atomic densities, sample temperature, etc, but modifies the coordinates according to the displacements related to individual I. It makes the comparison to the experimental curves, and returns the R-factor value associated to individual I.
- (iii) The probability of being selected for crossover is calculated based on the R-factor of the individual. An individual with a lower R-factor has a higher chance to be selected for the crossover process.

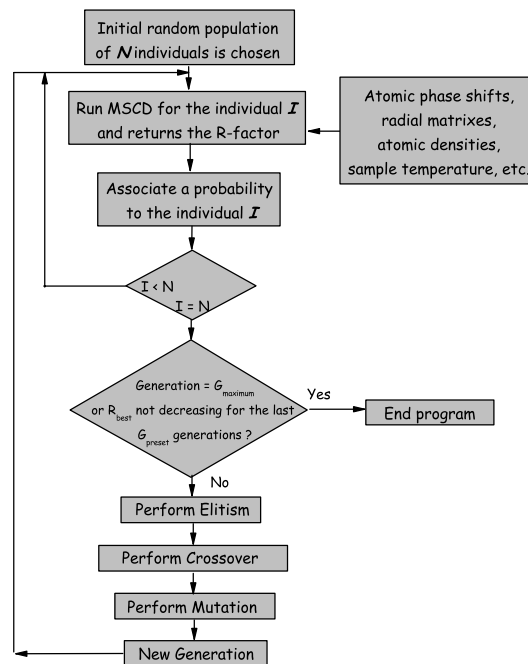


**Figure 1.** Schematic flow chart of the genetic algorithm implemented for photoelectron diffraction structural determination using the MSCD code.

- (iv) The steps (ii), and (iii) are repeated for all other individuals in the population.
- (v) The search stops here if the best R-factor has not decreased after a preset number of generations or if a preset maximum number of generations is reached: the best individual in the last generation is selected as the best solution. Otherwise, the best individual is cloned to the next generation (by elitism) and the process continues.
- (vi)  $N/2$  pairs of individuals are chosen according to probabilities based on their R-factors obtained in step (iii). The crossover process then creates  $N$  new individuals for the next generation. The worst one is discarded, being replaced by the clone obtained in the previous step.
- (vii) A number between 0 and 1 is chosen randomly. If this number is smaller than a previously chosen mutation rate, then a randomly chosen individual is subjected to the mutation process.
- (viii) The new generation is ready, and the process restarts at step (ii) for the new generation.

In the present calculations, we used a different stop criterion, because the solutions were already known from other studies. We also know that our present analysis method reproduces the prior solutions with good accuracy. So we know the best R-factors: 0.10 for Cu(111), 0.13 for Ag(111) and 0.05 for Ag(110)- $c(2 \times 2)$ -Sb. Thus, in the performance tests of the algorithm presented in the next section we have stopped the search when the GA finds a R-factor within 5% of the above mentioned values.

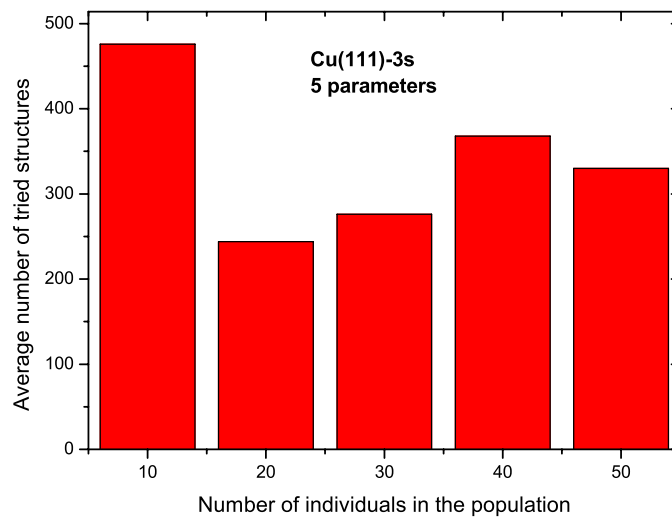


**Figure 2.** Average number of trial structures over eight different runs for populations with different sizes using the clean Cu(111) system.

### 3. Methodological results

The performance of the GA method depends on the choice of initial parameters. The mutation rate, the number of individuals to be cloned to the next generation and the number of individuals in each generation (population size) affect the speed of the search process. High mutation rates are not recommended, because of the randomness of the mutation process. Here, we permitted one out of one hundred individuals to undergo mutation, which prevents the search from becoming bound to local minima, without excessively randomizing the process. We have always cloned only the single best individual to the next generation, allowing the remaining ones to change by crossover. The correct choice for the population size  $N$  is not so clear: increasing the number of individuals means that a larger number of different starting points is investigated, and thus there is a higher probability of finding the global minimum in early generations. On the other hand, calculating theoretical photoelectron intensity curves for each individual requires much computational time and, in big populations, many of those calculations are not used to create new generations. A balance between these opposite effects is desirable.

We have therefore analyzed the number of structures that have to be investigated to find the global minimum for different population sizes. Due to the random nature of the initial population, an average over different runs is required. We performed calculations for populations with 10, 20, 30, 40, and 50 individuals, averaging over eight different initial populations for each of these populations. The clean Cu(111) system was used for these tests. Details of the experimental photoemission measurements used in the optimization procedure and discussion on the structural parameters obtained is provided in section 4. We optimized five parameters, namely, the first three interlayer spacings, the Debye temperature and the inner potential. Figure 2 shows the results. Twenty individuals appear to form a good population size: a sample with  $N = 20$  finds the global minimum by investigating a relatively small number of structures. Since the Cu(111) structure was previously known, we considered that the calculation was converged whenever the GA found the correct parameters within error bars of 5%. Figure 3 shows, for five particular illustrative runs with different population sizes, the



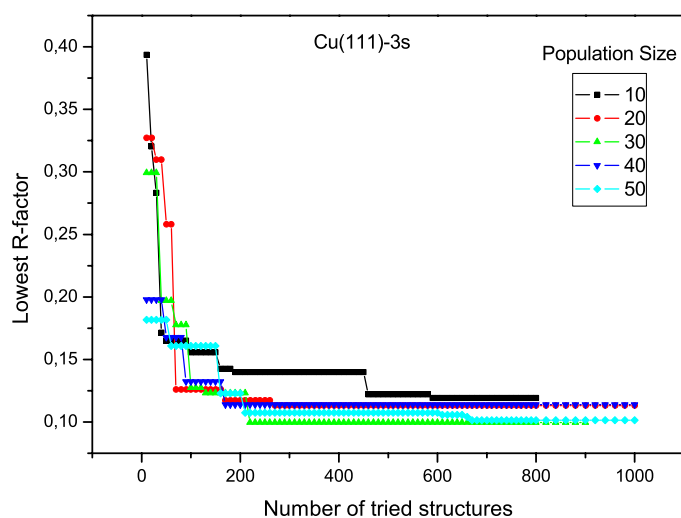


**Figure 3.** Best R-factor in each generation against the number of trial structures for the Cu(111) system. These are particular illustrative runs for different population sizes.

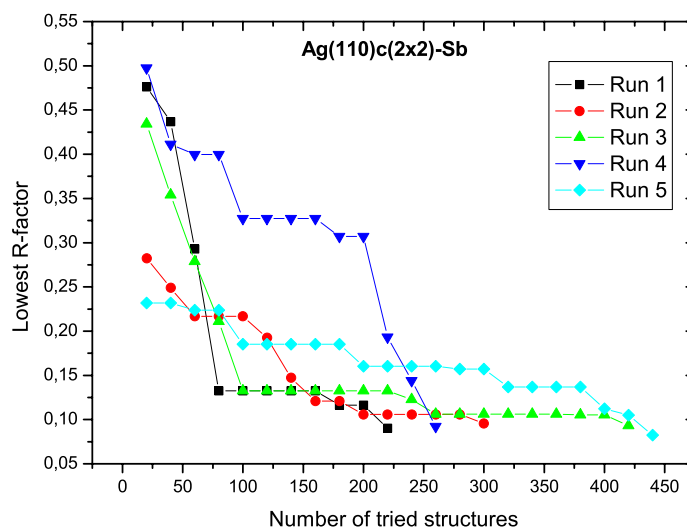


**Figure 4.** Best R-factor on each generation against the number of trial structures for the Ag(110)-c(2 × 2)-Sb system. These are particular illustrative runs for different initial populations, each consisting of 20 individuals.

R-factor of the best individual in each generation plotted against the number of previously tried structures for the Cu(111) system. As a general rule, larger values of  $N$  imply a lower final value of the R-factor.

Figure 4 shows the R-factor of the best individual for each generation for the Ag(110)-c(2 × 2)-Sb system, in which real codification was implemented. Five particular illustrative runs, all of them using 20 individuals in the population, are presented. When comparing the full circle/red curve (for 20 individuals) in figure 3 to the curves in figure 4 we can observe a similar behavior converging around 250 tried structures; however, in the second test six parameters

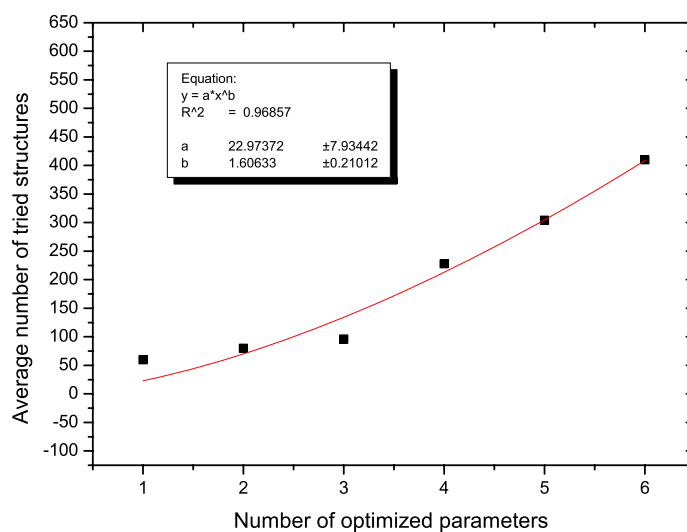


**Figure 5.** Scaling behavior for the genetic algorithm method applied to the photoelectron diffraction structural determination of the Ag(110)-c(2 × 2)-Sb system.

were fitted versus five in the first test, suggesting that the real codification showed a slightly better performance.

An important test to evaluate the performance of an optimization method is to analyze the way in which the number of trials needed to find the minimum increases when the number of parameters to be optimized grows. In other words, it is important to establish a scaling behavior for the method. For this purpose, we used compared theory to theory for the Ag(110)-c(2 × 2)-Sb system. We started with six parameters and determined the optimal values for the surface coordinates, which are shown in table 4 of section 4. Then we fixed the sixth coordinate in the optimal position and optimized five parameters. Keeping the fifth and the sixth coordinates fixed, we optimized four parameters and we proceeded in the same way for three, two and one parameter(s). For each number of optimized parameters we performed ten runs, starting from different initial populations and taking an average number of trial structures, as is shown in the figure 5. It can be observed that the number of trial structures is not a linear function of the number of optimized parameters if all points of the curve are taken into account. However, we can split the curve into two different regions, from one to three parameters (where a linear dependence is seen), and from four to six parameters (where the dependence is still linear but the slope is larger). Taking into account all points, a fitting to  $y = Ax^B$ , results in a exponent  $B = 1.6 \pm 0.2$ . In order to understand what this value means we can compare it with previous scaling factors obtained for LEED structural analysis. Direct-search algorithms exhibit approximately an  $N^2$  scaling [21], where  $N$  is the number of parameters. The first application of the simulated annealing method to the LEED problem performed by Rous [13] suggested an  $N^6$  scaling. The global search method proposed by Kottcke and Heinz [17] resulted in an  $N^{2.5}$  scaling. The work of Nascimento and co-workers [14, 15] concerning the fast simulated annealing approach, has obtained an  $N^1$  scaling. Döll and Van Hove have investigated the application of the genetic algorithm to the LEED problem [18], but the scaling behavior was not analyzed. We can conclude that the  $N^{1.6}$  scaling obtained for PED analysis in the present work is a satisfactory behavior for the computational time as a function of the number of parameters to be optimized. However, it is necessary to say that the scaling behavior

**Table 3.** Structural determination results for the Cu(111) system.

	GA-MSCD	ECT [23]	EAM [23, 26]	LEED [25]
Inner potential (eV)	3.5	—	—	—
Debye temperature (K)	450	—	216	—
$\Delta d_{12}$ (%)	-1.4	-3.1	-1.4	$-0.7 \pm 0.5$
$\Delta d_{23}$ (%)	-0.4	+1.9	-0.05	—
R-factor	0.10	—	—	$0.13 \pm 0.03$

**Table 4.** Structural determination results for the Ag(110)-c(2 × 2)-Sb system. The arrows for the *rumple* results indicate in which direction the Sb atoms move (up = out, down = in). The per cent values relate to the interlayer bulk distances.

Parameter	LEED [20]	GA-MSCD (theory versus theory)
$\Delta Z_{\text{AgSb}}$ ( <i>rumple</i> )	( $\downarrow 0.05 \pm 0.05$ ) Å ( $\downarrow 4.2\%$ )	$\downarrow 0.06$ Å ( $\downarrow 4.2\%$ )
$d_{12}(\Delta d_{12})$	( $1.37 \pm 0.04$ ) Å ( $-5.3\%$ )	1.37 Å ( $-5.3\%$ )
$d_{23}(\Delta d_{23})$	( $1.48 \pm 0.04$ ) Å ( $+2.5\%$ )	1.45 Å ( $+2.4\%$ )
$d_{\text{bulk}}$	1.4443 Å	1.4443 Å
$\Theta_{\text{D1}}$	( $160 \pm 60$ ) K	160 K
$\Theta_{\text{D2}}$	( $170 \pm 100$ ) K	160 K
$\Theta_{\text{bulk}}$	225 K	160 K

was performed using just ten different runs, and better statistics could present a different behavior.

#### 4. Structural determination results

In order to show that the genetic algorithm method can find the correct structural and non-structural surface parameters, we present, in this section, the results for the three analyzed systems, and we make a comparison with previous results for two of them.

The first tested structure was the clean Cu(111) surface. For this purpose, we used the energy-scanned experimental curves obtained by the group of Shirley<sup>5</sup>. Measurements were made at 80 K. The photoelectrons were excited from the Cu 3s core level using photons in the energy range 203.1–657.3 eV at normal incidence. Our theoretical simulation was performed using a cluster of 150 atoms, with eighth order of multiple scattering and second order of the Rehr–Albers separable representation. For this structure, five parameters were optimized: the first three interlayer spacings, the Cu Debye temperature and the inner potential. Table 3 shows the results obtained using our GA-MSCD fitting procedure and compares them to previous results: theoretical, namely ECT (equivalent crystal theory) [23] and EAM (embedded atom methods) [24], and experimental, namely LEED (low-energy electron diffraction) [25]. We note that the R-factors obtained in LEED and in GA-MSCD in table 3 are not directly comparable, as they are defined in different ways for the two methods. The R-factor for PED is defined in equation (1) and the definition for LEED can be found in [18]. The spacing changes  $\Delta d_{n,n+1}$  (%) shown in tables 3, 4, and 5 are relative to the bulk interlayer spacing of Cu(111), Ag(110), and Ag(111) respectively. Good agreement with previous results for some structural parameters is found: in particular, there is a small contraction of the spacing between the first and the second atomic layers. The same agreement is not found for the Debye temperature. Nevertheless, it is necessary to remember that the MSCD package defines a cluster Debye temperature, different from others approaches that treat the Debye temperature in the bulk and

<sup>5</sup> The data were obtained by the group of D A Shirley in the Advanced Light Source of Lawrence Berkeley National Laboratory, and are included in the documentation of the MSCD package. See [22].

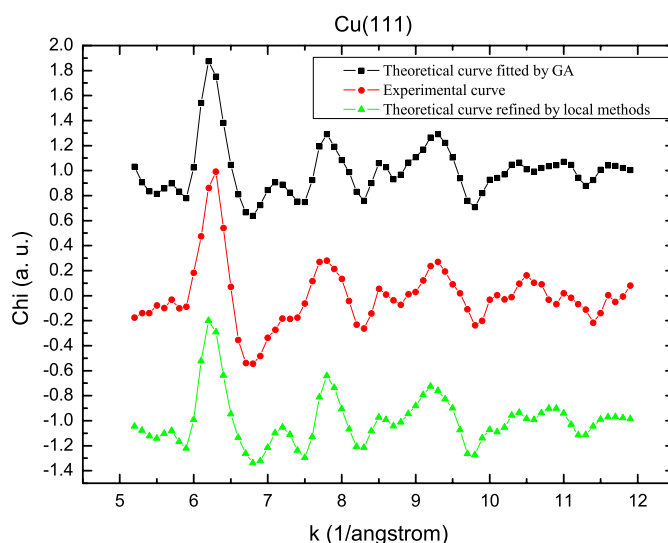


**Figure 6.** Normalized PED intensities ( $\chi$  functions) for the Cu(111) system. The first curve was theoretically generated by the MSCD code from the structure found by the GA; the second is the experimental one; the third curve, theoretical, is a further local optimization starting from the structure found by the GA, used to test the local optimization of the GA search itself.

**Table 5.** Structural determination results for the Ag(111) system.

	GA-MSCD	ECT [23]	EAM [23, 26]	LEED [28]	DFT [27]
Inner potential (eV)	4.36	—	—	—	—
Debye temperature (K)	130	—	143	160	—
$\Delta d_{12}$ (%)	-0.8	-2.5	-1.3	$-(0.5 \pm 0.4)$	-0.3
$\Delta d_{23}$ (%)	+0.1	+1.6	-0.04	$-(0.4 \pm 1.2)$	0.04
R-factor	0.13	—	—	0.18	—

the outermost layers separately. To verify our implementation of the GA and its convergence, we performed, after the global GA optimization, a separate local optimization starting from the structure found by the GA. The R-factor did not decrease, showing that, at least for this simple system, the GA was able to find not only the deeper well, as was expected, but also the minimum inside the well. Figure 6 shows the  $\chi$  function, or the normalized PED intensity from which was subtracted the background intensity for the experimental curve, as well as for the simulated curve obtained by the GA fitting procedure and for the simulated curve obtained after the refinement through local methods. As it was mentioned before, the refinement did not make the R-factor decrease, because the simulated curves in figure 6 are so similar. This is a remarkable example of the efficiency of the GA procedure, that it is not only able to find the global minimum, but also locally reaches the best fitting parameters with high accuracy.

In order to establish a scaling behavior for the GA method, described in the previous section, we performed a second test using a theory–theory comparison for the Ag(110)-c(2 × 2)-Sb system. In a theory–theory comparison the method should be able to obtain an R-factor equal to or very near to zero. Nascimento *et al* [20] have performed a structural analysis by LEED for the Ag(110)-c(2 × 2)-Sb system, exploring six different structural models for 0.5 monolayers of Sb on a Ag(110) substrate. Their results showed that the substitutional first layer model (shown in figure 7) best fits the experimental data; its structural parameters are

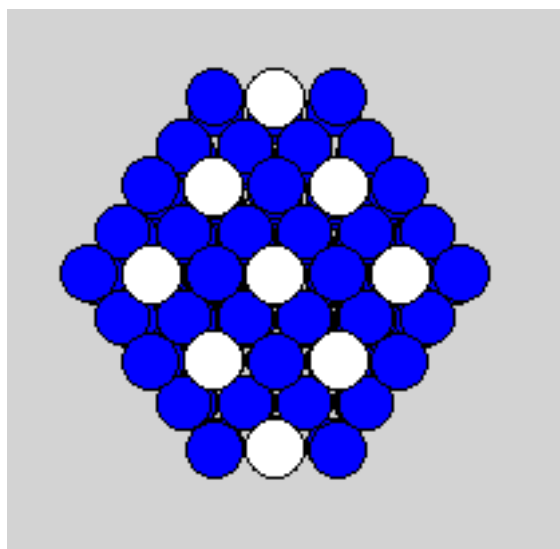


**Figure 7.** First layer substitutional model for 0.5 monolayers of Sb (white circles) deposited on the Ag(110) (dark/blue circles) substrate.

presented in table 4. Therefore we used the LEED results as the input structure for an MSCD calculation to create ‘pseudo-experimental’ angular scan PED curves for polar angles varying from  $5^\circ$  to  $80^\circ$  with a step of  $5^\circ$  and azimuthal angles varying from  $0$  to  $90^\circ$  with a step of  $3^\circ$ . We performed this simulation using a cluster of 180 atoms. We simulated photoelectrons being excited from several different core levels, but the Sb 3d level excited by a simulated radiation source of 600 eV showed the greatest sensitivity to the surface structural parameters. Therefore, we used only this level in our calculations (as could also be done in the experiment). We used eighth order of multiple scattering and second order of Rehr–Albers separable representation. Once the ‘pseudo-experimental’ PED curves were simulated we started the GA search process from the bulk values for the surface parameters, placing the Sb atoms at the same positions as the Ag atoms which they replace. After about 400 trials the GA could find the correct values with a very good accuracy, obtaining an R-factor of 0.04. The structural parameters are presented in table 4. Figure 8 shows the ‘pseudo-experimental’ pattern and the one found by the GA. A very good agreement between the patterns can be seen.

The third test performed was for clean Ag(111). For this system, experimental angular scans are available; the experiment was performed at room temperature<sup>6</sup>. The photoelectrons were excited from the Ag 3d core level by 750 eV photons. The scans were performed for polar angles varying from  $15^\circ$  to  $55^\circ$ , with a step of  $5^\circ$ , and azimuthal angles from  $0^\circ$  to  $129^\circ$ , with step of  $3^\circ$ . The theoretical simulation was performed using a cluster of 200 atoms, eighth order of multiple scattering, and second order of Rehr–Albers separable representation. For this structure, five parameters were optimized: the three first interlayer spacings, the cluster Debye temperature and the inner potential. We found good agreement with previous results for this system. Table 5 compares our results to the previous ones obtained by ECT (equivalent crystal theory), EAM (embedded atom methods), LEED (low-energy electron diffraction), and DFT (density functional theory) [27]. In figure 9, we can see the nice agreement between the experimental and calculated PED diffraction patterns.

<sup>6</sup> Laboratório Nacional de Luz Síncrotron, Campinas-SP, Brazil.

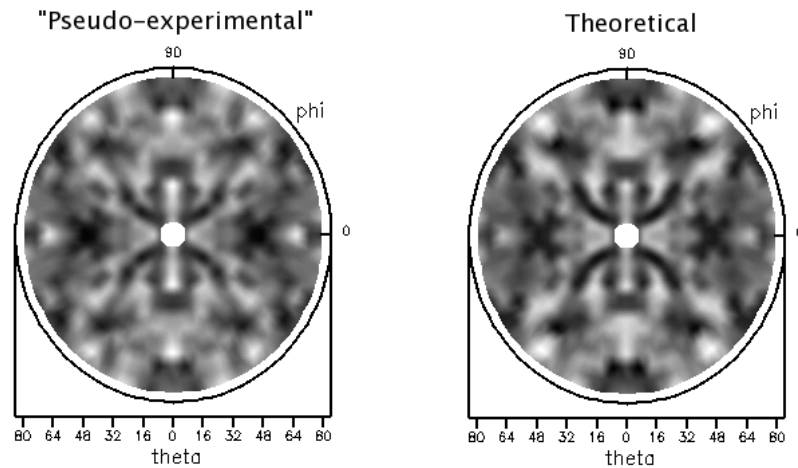


**Figure 8.** ‘Pseudo experimental’ (left) and calculated (right) PED diffraction patterns for Sb 3d emission from the Ag(110)-c(2 × 2)-Sb system. The angles  $\theta$  and  $\phi$  are the polar and azimuthal angles between the analyzer and the sample. The white holes at the centers of the figures result from starting the simulations at  $\theta = 3^\circ$ .

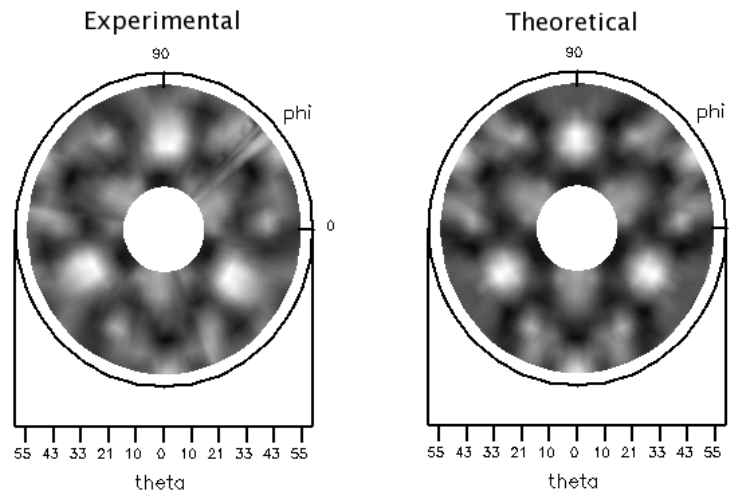


**Figure 9.** Experimental (left) and calculated (right) PED diffraction patterns for the Ag 3d emitter for the clean Ag(111) system. The angles  $\theta$  and  $\phi$  are the polar and azimuthal angles between the analyzer and the sample. The white holes at the center of the figures arise because the simulations were performed beginning at  $\theta = 15^\circ$ .

## 5. Summary and conclusions

Surface atomic structural determination by photoelectron diffraction relies on theoretical simulation for reliable and accurate results. Especially for complex surface structures, global optimization methods are necessary to fit the theoretical to the experimental curves. In this paper, we have explored the use of the GA procedure to reach this goal. The speed of the optimization process depends on an adequate choice of the initial GA parameters, such as population size and mutation and elitism rates. Three structures were successfully solved using the GA approach: clean Cu(111), Ag(110)-c(2 × 2)-Sb and Ag(111). We have compared the

performance of the GA with local optimization methods for the first and third systems. We note that the R-factor obtained is similar. We may conclude that the combination of global search methods, such as GA, and efficient photoelectron diffraction codes, such as the MSCD package, can be extremely useful in the determination of surface structures from photoelectron diffraction experimental data. This is of particular importance for complex surfaces, in which many structural parameters are needed to describe the complete surface structure.

### Acknowledgments

The authors would like to thank Fundação de Amparo à Pesquisa de Estado de Minas Gerais (FAPEMIG), Conselho Nacional de Desenvolvimento Científico e Tecnológico (CNPQ), and Coordenação de Aperfeiçoamento de Pessoal de Nível Superior (CAPES) (Brazilian Research Agencies) for financial support. MAVH was supported by City University of Hong Kong Grant No. 9380041.

### References

- [1] Fadley C S 2005 *Nucl. Instrum. Methods Phys. Res. A* **547** 24–41
- [2] Osterwalder J, Aebi P, Fasel R, Naumovic D, Schwaller P, Kreuz T, Schlapbach L, Abukawa T and Kono S 1995 *Surf. Sci.* **331** 1002–14
- [3] Fadley C S, Chen Y, Couch R E, Daimon H, Denecke R, Denlinger J D, Galloway H, Hussain Z, Kaduwela A P, Kim Y J, Len P M, Liesegang J, Menchero J, Morais J, Palomares J, Ruebush S D, Rotenberg E, Salmeron M B, Scalettar R, Schattke W, Singh R, Thevuthasan S, Tober E D, Van Hove M A, Wang Z and Ynzunza R X 1997 *Prog. Surf. Sci.* **54** 341–87
- [4] Schattke W, Van Hove M A, García de Abajo F J, Díez Muiño R and Mannella N 2003 *Solid-State Photoemission and Related Methods: Theory and Experiment* ed W Schattke and M A Van Hove (Berlin: Wiley-VCH) chapter 2, pp 50–114
- [5] Gunnella R, Solal F, Sébilleau D and Natoli C R 2000 *Comput. Phys. Commun.* **132** 251–66
- [6] Harp G R, Ueda Y, Chen X and Saldin D K 1998 *Comput. Phys. Commun.* **112** 80–90
- [7] García de Abajo F J, Van Hove M A and Fadley C S 2001 *Phys. Rev. B* **63** 075404-1–16
- [8] The EDAC online is available at <http://csic.sw.edu.es/jga/software/edac>
- [9] The MSCD program package is available at <http://www.sitp.lbl.gov/mscdpack>
- [10] Chen Y, García de Abajo F J, Chassé A, Ynzunza R X, Kaduwela A P, Van Hove M A and Fadley C S 1998 *Phys. Rev. B* **58** 13121
- [11] Rehr J J and Albers R C 1990 *Phys. Rev. B* **41** 8139
- [12] Zhao Z, Meza J C and Van Hove M A 2006 *J. Phys.: Condens. Matter* **18** 8693–706
- [13] Rous P J 1993 *Surf. Sci.* **296** 358
- [14] Nascimento V B, de Carvalho V E, de Castilho C M C, Soares E A, Bittencourt C and Woodruff D P 1999 *Surf. Rev. Lett.* **5** 651
- [15] Nascimento V B, de Carvalho V E, de Castilho C M C and Soares E A 2001 *Surf. Sci.* **487** 15
- [16] Nascimento V B, Soares E A, de Carvalho V E, Lopes E L, Paniago R and de Castilho C M C 2003 *Phys. Rev. B* **68** 245408
- [17] Kottcke M and Heinz K 1997 *Surf. Sci.* **376** 352
- [18] Döll R and Van Hove M A 1996 *Surf. Sci.* **335** L393–8
- [19] Scales J A, Smith M L and Fischer T L 1992 *J. Comput. Phys.* **103** 258–68
- [20] Nascimento V B, Paniago R, de Siervo A, de Castilho C M C, Landers R, Soares E A and de Carvalho V E 2004 *Surf. Sci.* **572** 337–46
- [21] Rous P J, Van Hove M A and Somorjai G A 1990 *Surf. Sci.* **226** 15
- [22] <http://www.sitp.lbl.gov/mscdpack>
- [23] Smith J R, Perry T, Banerjee A, Ferrante J and Bozzolo G 1991 *Phys. Rev. B* **44** 6444
- [24] Daw M S and Baskes M I 1984 *Phys. Rev. B* **29** 6443–53
- [25] Lindgren S A, Wallden L, Rundgren J and Westrin P 1984 *Phys. Rev. B* **29** 576
- [26] Al-Rawi A N, Kara A and Rahman T S 2002 *Phys. Rev. B* **66** 165439
- [27] Wang Y, Wang W, Fan K-N and Deng J 2001 *Surf. Sci.* **490** 125–32
- [28] Soares E A, Leatherman G S, Diehl R D and Van Hove M A 2000 *Surf. Sci.* **468** 129–36